

*Master in Photonics*

**MASTER THESIS WORK**

**Stability and dynamics of a two-component  
Bose-Einstein condensate in ring ladders**

**Eulàlia Nicolau Jiménez**

**Supervised by Dr. Verònica Ahufinger, (UAB)**

Presented on date 19<sup>th</sup> July 2018

Registered at

 **ETSETB**

**Escola Tècnica Superior  
d'Enginyeria de Telecomunicació de Barcelona**

# Stability and dynamics of a two-component Bose-Einstein condensate in ring ladders

**Eulàlia Nicolau Jiménez**

Grup d'Òptica. Departament de Física. Universitat Autònoma de Barcelona,  
Barcelona E-08193, Spain

E-mail: eulalia.nicolau@gmail.com

**Abstract.** We investigate the dynamics of a two-component Bose-Einstein condensate trapped in two coupled rings in ladder configuration. First, we derive from the two-component Gross-Pitaevskii equation a few state model for the angular momentum modes. Then, we analyse the stability of the stationary states by solving the Bogoliubov-de Gennes equations. Also, we study the dynamics of the system for an arbitrary population imbalance between the rings, characterizing the transition from Josephson oscillations to quantum self-trapping. We also derive the self-trapping condition for the bosonic mixture, finding simultaneous self-trapping of the two components.

*Keywords:* Two-component Bose-Einstein condensate, toroidal potential, Bogoliubov spectrum, Josephson oscillations, self-trapping.

## 1. Introduction

Ring potentials are one of the most promising geometries in the emerging field of atomtronics [1], and they are instrumental in many quantum sensing implementations, such as Sagnac interferometry [2] or the atomic analogue of the superconductor device SQUID [3]. These are the simplest geometries that lead to non-trivial loop circuits, in which the superfluidity of Bose-Einstein condensates (BECs) acquires a fundamental role, allowing the appearance of persistent currents as well as vortices. In these systems, orbital angular momentum can be transferred to the ultracold atoms either by rotating a weak link [4] or by coherent transfer of angular momentum from light to the atoms [5]. Several techniques to generate these potentials have been proposed: optical plugged magnetic traps [6], conical refraction [7], static Laguerre-Gauss Beams [8], and time-averaged [9, 10, 11] or painting [12, 13] potentials.

On the other hand, tunnelling is a paradigm of quantum mechanics and a particular topic of interest in the field of ultracold atoms. The dynamics of BECs in tunnel-coupled ring geometries have been thoroughly explored for a variety of geometries such as ladder ring structures with [14] or without lattices [15], or concentric rings [16, 17].

In this work, we focus on bosonic binary mixtures, which comprise two species of bosons, either from different hyperfine states [18], isotopes [19] or atoms [20]. In these cases, the ratio between the intra- and inter-species interactions gives rise to a miscible and a phase-segregated regime, which leads to new phenomenology, *e.g.* the emergence of classical rotation in toroidal potentials [21]. Recently, tunnelling dynamics have been studied for binary mixtures for the case of concentric rings [22], including the case of dipolar interactions [23]. Here, we investigate a two-ring ladder trap with a two-component BEC in the miscible regime in order to explore the interplay between the tunnelling dynamics, the angular momentum, and the nonlinear interactions.

The paper is organized as follows. In section 2, we describe the physical system, and in section 3, we derive from the two-component Gross-Pitaevskii equation (TCGPE) a few state model in terms of the angular momentum modes. In section 4, we study the Bogoliubov-de Gennes perturbations in the stationary states to identify their regions of stability. In section 5, we analyse the phase boundary between the quantum self-trapping and the Josephson oscillations regimes. The analytical results are corroborated by numerical integration of the complete set of equations that describe the system. Finally, we present the conclusions in section 6.

## 2. Physical system

The considered system is shown in figure 1. It consists of two coaxial annular traps around the  $z$ -axis separated by a distance  $2z_0$ , where a two-component BEC is trapped.

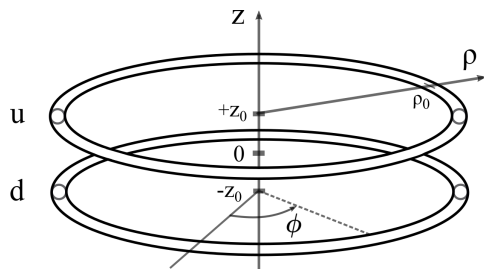


**Figure 1.** Schematic representation of the geometry of the system. The potential consists of two ring traps centered at  $\rho = 0$ , in the planes  $\pm z_0$  with radius  $\rho_0$ , formed by a radial harmonic potential  $V_\rho$  and a double well potential in  $z$ ,  $V_z$ .

The bosonic mixture considered in this work is described within the mean field theory by the TCGPE, that written in cylindrical coordinates reads [24, 25]

$$i\hbar \frac{\partial \Psi_j(\mathbf{r})}{\partial t} = \left[ \frac{\hbar^2}{2M} \left( -\frac{\partial^2}{\partial \rho^2} - \frac{\partial^2}{\partial z^2} + \frac{L_z^2}{\hbar^2 \rho^2} \right) + V_{ext}(\mathbf{r}) + g_{jj} |\Psi_j(\mathbf{r})|^2 + g_{ji} |\Psi_i(\mathbf{r})|^2 \right] \Psi_j(\mathbf{r}). \quad (1)$$

The wavefunctions of each component are  $\Psi_j(\mathbf{r})$ , where  $j, i = 1, 2$  and  $j \neq i$ ,  $V_{ext}(\mathbf{r})$  is the external potential,  $M \equiv m_1 = m_2$  is the atomic mass, and the constants  $g_{ji}$  characterize the nonlinear interactions. In (1), the term  $\frac{1}{\rho} \frac{\partial}{\partial \rho}$  has been neglected, as the radius of the rings is large compared to the variation of the wavefunctions in  $\rho$ , and  $L_z = -i\hbar \frac{\partial}{\partial \phi}$  is the

$z$  component of the angular momentum. The TCGPE can be obtained from the second quantization manybody hamiltonian assuming weak interactions and a large number of particles; in that case, quantum and thermal fluctuations can be neglected in the limit  $T = 0$ , such that the boson field operator can be approximated by its expected value. Next, we describe the different terms in the TCGPE, (1).

The nonlinear terms in (1) describe contact interactions, as these predominate in cold and dilute gases, and include the intra-species interactions, which are considered equal for both components ( $g_{11} = g_{22}$ ), and the inter-species interactions  $g_{ji}$  ( $i \neq j$ ). Each one is characterized by a single parameter, the  $s$ -wave scattering length  $a_{ji}$ , such that  $g_{ji} = 4\pi\hbar^2 a_{ji}/M$ . The ground state of this mixture exhibits two phases depending on the ratio between the inter- and intra-species interactions: the miscible regime, in which the wavefunctions of the two components overlap, and the immiscible regime, in which there is phase separation. The miscibility condition can be derived from the time-independent TCGPE imposing stability on the homogeneous solution, (*i.e.*, for  $V_{ext}(\mathbf{r}) = 0$ ), which leads to the following two conditions [26]

$$g_{11}, g_{22} > 0, \quad \text{and} \quad g_{11}g_{22} > g_{12}^2. \quad (2)$$

If these conditions are not fulfilled, the ground state of the system is in the phase separated regime. Henceforth, we will consider exclusively repulsive interactions in the miscible regime.

The trapping potential in (1) is defined as  $V_{ext}(\mathbf{r}) = V_\rho(\rho - \rho_0) + V_z(z, z_0)$ , where  $V_z$  is a symmetric double well potential with minima at  $\pm z_0$ , and  $V_\rho$  is an harmonic radial potential centered at  $\rho_0$ . The external potentials  $V_z$  and  $V_\rho$  are steep enough so that the energy level separation is large and only the ground states are populated. Assuming also weak coupling between the two wells, the wavefunction in  $z$  is well approximated by the sum of the two ground states. Therefore, the wavefunction of each component can be factorized as

$$\Psi_j(\mathbf{r}) = \Psi_j^\rho(\rho) [\Phi_j(z - z_0)\chi_j^u(\phi) + \Phi_j(z + z_0)\chi_j^d(\phi)] \equiv \Psi_j^\rho [\Phi_j^u\chi_j^u + \Phi_j^d\chi_j^d], \quad (3)$$

where  $\Psi_j^\rho(\rho)$  is the ground state of the radial harmonic potential,  $\Phi_j^{u/d}$  are the harmonic ground states of the lower ( $d$ ) and upper ( $u$ ) well of the double well potential, respectively, and the functions  $\chi_j^{u/d}(\phi)$  contain the dependence of the BECs wavefunction with respect to the azimuthal angle,  $\phi$ . As we are studying the miscible regime, the ground states in  $\rho$  and  $z$  are equal in both components:  $\Psi_j^\rho = \Psi_i^\rho \equiv \Psi^\rho$  and  $\Phi_j^{u/d} = \Phi_i^{u/d} \equiv \Phi^{u/d}$ . For a BEC with weak interactions, the wavefunctions in  $\rho$  and  $z$  are well approximated by harmonic wavefunctions:

$$\Psi^\rho(\rho) = \left(\frac{1}{\sqrt{\pi}a_\rho}\right)^{1/2} e^{-(\rho-\rho_0)^2/2a_\rho^2} \quad \text{and} \quad \Phi(z \pm z_0) = \left(\frac{1}{\sqrt{\pi}a_z}\right)^{1/2} e^{-(z \pm z_0)^2/2a_z^2}, \quad (4)$$

where  $a_\rho$  and  $a_z$  are the harmonic oscillator lengths of the ground states which are taken as equal,  $a_\rho = a_z$ . The functions  $\chi_j^{u/d}(\phi)$  for the upper and lower rings can be written as a conveniently normalized linear combination of the angular momentum eigenstates:

$$\chi_j^{u/d} = \frac{1}{\sqrt{2\pi}} e^{i\theta_j^{u/d}} \sum_{m=-\infty}^{\infty} \alpha_{m,j}^{u/d} e^{im\phi}, \quad (5)$$

with amplitudes  $\alpha_{m,j}^{u/d}$ , where  $\theta_j^{u/d}$  is the phase of the wavefunction in each ring. For each eigenstate, the condensate has a quantized angular momentum  $m\hbar$ .

### 3. Angular momentum coupled-mode equations

We will now proceed to derive the evolution equations for the angular momentum modes in each ring and component, generalizing the model obtained by I. Lesanovsky and W. von Klitzing [15] for a single-component BEC. First, we shall introduce the factorized wavefunction, (3), into the cylindrical TCGPE, (1), and integrate out the dependence on  $\rho$  and  $z$  in order to obtain the evolution of  $\chi_j^{u/d}(\phi)$ . We project over  $(\Psi^\rho)^*$  and integrate for all values of  $\rho$ , and then we project over  $(\Phi^d)^*$  and integrate over all  $z$ . Using the orthonormality of the states in  $z$  and  $\rho$ , ( $\int (\Psi^\rho)^* \Psi^\rho d\rho = 1$  and  $\int dz (\Phi^a)^* \Phi^b = \delta_{ab}$  with  $a, b = u, d$ ), one obtains

$$i\hbar \frac{\partial \chi_j^d}{\partial t} = \frac{\hbar^2}{2M} \left[ - \int dz (\Phi^d)^* \frac{\partial^2 \Phi^u}{\partial z^2} \chi_j^u - \frac{1}{R^2} \frac{\partial^2 \chi_j^d}{\partial \phi^2} \right] + \left( \int d\rho |\Psi^\rho|^4 \int dz |\Phi|^4 \right) (g_{jj} |\chi_j^d|^2 + g_{ji} |\chi_i^d|^2) \chi_j^d + \int dz (\Phi^d)^* V_z \Phi^u \chi_j^u + E_k^{z,d} \chi_j^d + E_k^\rho \chi_j^d + E_P^{z,d} \chi_j^d + E_P^\rho \chi_j^d, \quad (6)$$

where  $\int dz |\Phi^u|^4 = \int dz |\Phi^d|^4 \equiv \int dz |\Phi|^4$  and we have defined the factor  $\frac{1}{R^2} = \int d\rho \rho^{-2} |\Psi^\rho|^2$ . The kinetic and potential energies in  $\rho$  and  $z$  are defined as

$$E_k^\rho \equiv -\frac{\hbar^2}{2M} \int d\rho (\Psi^\rho)^* \frac{\partial^2 \Psi^\rho}{\partial \rho^2}, \quad \text{and} \quad E_P^\rho \equiv \int d\rho (\Psi^\rho)^* V_\rho \Psi^\rho \quad (7)$$

$$E_k^{z,d} = -\frac{\hbar^2}{2M} \int dz (\Phi^d)^* \frac{\partial^2 \Phi^d}{\partial z^2}, \quad \text{and} \quad E_P^{z,d} = \int dz (\Phi^d)^* V_z \Phi^d. \quad (8)$$

These terms produce a shift in the energy of the system without altering its dynamics, therefore they can be set to zero for simplicity. The evolution equation for  $\chi_j^u$  can be obtained following an analogous procedure to the one described above. To rewrite (6) and its analogue for  $\chi_j^u$  in a more compact form, we define the following parameters:

$$\tau = \frac{\hbar}{2MR^2} t, \quad \kappa = R^2 \int dz \Phi^d \left[ \frac{\partial^2}{\partial z^2} - \frac{2M}{\hbar^2} V_z \right] \Phi^u, \quad \gamma_{ji} = \frac{2MR^2 g_{ji}^{1D}}{\hbar^2}, \quad (9)$$

where  $\tau$  is the scaled time,  $\kappa$  is the coupling coefficient that characterizes the tunnelling between the two rings, and  $\gamma_{ji}$  is the interatomic interaction parameter, where  $g_{ji}^{1D}$  is the 1D nonlinear constant,  $g_{ji}^{1D} = g_{ij} \int d\rho |\Psi_j^\rho|^4 \int dz |\Phi|^4 = 2\hbar^2 a_s / M a_\rho^2$ . With the above definitions, (6) and its analogue for  $\chi_j^u$  simplify to the dimensionless form

$$i \frac{\partial \chi_j^{u/d}}{\partial \tau} = - \frac{\partial^2 \chi_j^{u/d}}{\partial \phi^2} - |\kappa| \chi_j^{d/u} + \gamma_{jj} |\chi_j^{u/d}|^2 \chi_j^{u/d} + \gamma_{ji} |\chi_i^{u/d}|^2 \chi_j^{u/d}. \quad (10)$$

Once the coupled equations for  $\chi_j^{u/d}(\phi)$  have been obtained, we can introduce their expansion in terms of angular momentum modes, (5), into (10) to obtain the coupled

equations for  $\alpha_{m,j}^{u/d}$  that describe the evolution of each angular momentum amplitude. Projecting over  $\exp(-im'\phi)$  and integrating over  $\phi$ , we obtain the following infinite set of nonlinear coupled equations (see details in Supplementary Material A):

$$i\frac{\partial\alpha_{m,j}^{u/d}}{\partial\tau} = m^2\alpha_{m,j}^{u/d} - |\kappa|\alpha_{m,j}^{d/u} + \frac{\gamma_{jj}}{2\pi} \sum_{nn'} \alpha_{n,j}^{u/d} (\alpha_{n',j}^{u/d})^* \alpha_{m-n+n',j}^{u/d} + \frac{\gamma_{ji}}{2\pi} \sum_{nn'} \alpha_{n,i}^{u/d} (\alpha_{n',i}^{u/d})^* \alpha_{m-n+n',j}^{u/d}. \quad (11)$$

The angular mode coefficients are normalized to the number of particles in the  $m$ -th angular mode in each ring for each component  $j$ ,  $|\alpha_{m,j}^{u/d}|^2 = N_{m,j}^{u/d}$ , such that the total number of particles in each ring and component is  $\int d\phi |\chi_j^{u/d}|^2 = N_j^{u/d}$ . The first term of the RHS in (11) corresponds to the kinetic energy of the  $m$ -th mode, the second term, to the tunnelling between the two rings, which only couples modes with the same  $m$ , and the third and fourth terms are the intra- and inter-species nonlinear interactions that couple different angular momentum modes within each ring. To solve the system of equations numerically, one has to truncate it at a large enough  $m$  to ensure that all the modes involved in the dynamics are considered.

#### 4. Stability of stationary solutions

For time-independent external potentials, one-component BECs have stationary solutions of the form  $\Psi(\mathbf{r}, t) = \Psi(\mathbf{r}) e^{-i\mu t/\hbar}$ , where the phase of the wavefunction is governed by the chemical potential  $\mu$ . One can study the stability of these states by adding a small perturbation to the solution in the Gross-Pitaevskii equation, which leads to the Bogoliubov-de Gennes equations [27]. In this section we study the stability of the angular momentum stationary solutions of our bosonic mixture.

##### 4.1. Stationary solutions

We are interested in solutions where only one angular momentum mode  $n$ , the same for both components, is initially populated:  $|\alpha_{n,j}^{u/d}|^2 = N_{n,j}^{u/d}$ ,  $|\alpha_{m \neq n,j}^{u/d}|^2 = 0$ . Stationary solutions only exist for equal number of particles between rings, and we impose for simplicity that both components have the same number of particles:  $N_{n,j}^{u/d} = N_{n,i}^{u/d} \equiv N$ . Then, (11) simplifies to

$$i\frac{\partial\alpha_{n,j}^{u/d}}{\partial\tau} = n^2\alpha_{n,j}^{u/d} - |\kappa|\alpha_{n,j}^{d/u} + \epsilon\alpha_{n,j}^{u/d} + \epsilon'\alpha_{n,j}^{u/d}, \quad (12)$$

where  $\epsilon = \gamma_{jj}N/(2\pi)$ , and  $\epsilon' = \gamma_{ij}N/(2\pi)$ . By diagonalizing this system of equations we find two stationary solutions

$$\alpha_{n,1}^u = \alpha_{n,1}^d \quad \text{and} \quad \alpha_{n,2}^u = \alpha_{n,2}^d \quad \text{with} \quad \mu_+ = n^2 + \epsilon + \epsilon' - |\kappa| \quad (13)$$

$$\alpha_{n,1}^u = -\alpha_{n,1}^d \quad \text{and} \quad \alpha_{n,2}^u = -\alpha_{n,2}^d \quad \text{with} \quad \mu_- = n^2 + \epsilon + \epsilon' + |\kappa|, \quad (14)$$

with  $\alpha_{n,j}^{u/d} = \pm\sqrt{N}e^{-i\mu\tau}$ . Thus, there is a stationary state which is symmetric (13) with respect to the upper and lower wells and a state which is antisymmetric (14). Note that the phase difference between the two components does not play a role.

#### 4.2. Excitation branches

In order to study the stability of these states, we add a small amplitude perturbation  $\delta\alpha_j$  in mode  $m$  of both components to the stationary state with  $n = 0$ , so that the perturbed state  $\tilde{\alpha}_{0,j}^{u/d}$  reads

$$\tilde{\alpha}_{0,j}^{u/d} = \alpha_{0,j}^{u/d} + \delta\alpha_j = \pm\sqrt{N}e^{-i\mu\tau} + e^{-i\mu\tau}(u_{m,j}^{u/d}e^{-i\omega\tau} + (v_{m,j}^{u/d})^*e^{i\omega\tau}). \quad (15)$$

By introducing this Ansatz into (11) and linearising for small amplitudes of  $u_{m,j}^{u/d}$  and  $(v_{m,j}^{u/d})^*$ , we obtain the following eigenvalue equations (Supplementary Material B)

$$\begin{aligned} \omega u_{m,j}^{u/d} &= (m^2 - \mu + 2\epsilon + \epsilon')u_{m,j}^{u/d} + \epsilon v_{-m,j}^{u/d} - |\kappa|u_{m,j}^{d/u} + \epsilon'(u_{m,i}^{u/d} + v_{-m,i}^{u/d}) \\ -\omega v_{-m,j}^{u/d} &= (m^2 - \mu + 2\epsilon + \epsilon')v_{-m,j}^{u/d} + \epsilon u_{m,j}^{u/d} - |\kappa|v_{-m,j}^{d/u} + \epsilon'(u_{m,i}^{u/d} + v_{-m,i}^{u/d}). \end{aligned} \quad (16)$$

Diagonalizing this system of equations we find 4 excitation branches for each state  $\mu_{\pm}$

$$\begin{aligned} \omega_{1,\pm} &= m\sqrt{m^2 + 2\epsilon + 2\epsilon'} & \omega_{3,\pm} &= \sqrt{(m^2 \pm 2|\kappa|)(m^2 - 2\epsilon' + 2\epsilon \pm 2|\kappa|)} \\ \omega_{2,\pm} &= m\sqrt{m^2 + 2\epsilon - 2\epsilon'} & \omega_{4,\pm} &= \sqrt{(m^2 \pm 2|\kappa|)(m^2 + 2\epsilon' + 2\epsilon \pm 2|\kappa|)}. \end{aligned} \quad (17)$$

For real values of  $\omega_{a,\pm}$  ( $a = 1, 2, 3, 4$ ), the perturbations in (15) remain periodic and thus bounded, whereas for imaginary values, the perturbations in mode  $m$  grow exponentially, destabilizing the stationary state. For repulsive interactions in the miscible regime (*i.e.*,  $\epsilon' < \epsilon$  with  $\epsilon, \epsilon' > 0$ ), the symmetric state (13) is stable against perturbations to higher order modes, as all the excitation branches  $\omega_{a,+}$  take real values in all the parameter space. For the antisymmetric state (14), the branches  $\omega_{3,-}$  and  $\omega_{4,-}$  can take imaginary values, rendering the state unstable. Figure 2 shows the real (blue dashed lines) and imaginary (red continuous lines) values of  $\omega_{4,-}$  as a function of  $|\kappa|$  for  $\epsilon = 1$  and a)  $\epsilon' = 0$ , b)  $\epsilon' = 0.4$ , c)  $\epsilon' = 0.8$ . Both the repulsive inter- and intra-species nonlinear interactions increase the instability regions of the antisymmetric state. The excitation branch  $\omega_{3,-}$  presents a similar profile wherein the instability regions are always smaller and included in those of  $\omega_{4,-}$ ; hence, it is the latter that determines the stability conditions of this state. The spectrum in (17) also holds for stationary solutions with  $n \neq 0$ , in which the perturbation  $m$  is the angular momentum with respect to  $n$ .

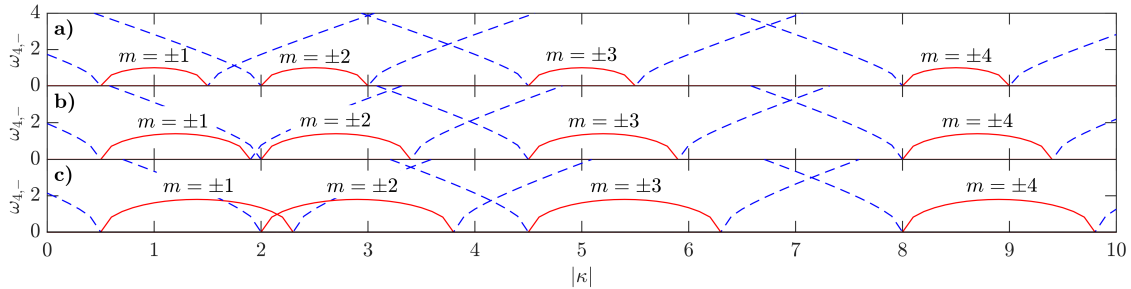


**Figure 2.** (color online).  $\omega_{4,-}$  branch of the Bogoliubov spectrum of the antisymmetric state for  $\epsilon = 1$ ,  $m = 1, 2, 3, 4$ , and different values of the inter-species nonlinear energy a)  $\epsilon' = 0$ , b)  $\epsilon' = 0.4$ , c)  $\epsilon' = 0.8$ . Red continuous lines: imaginary values; blue dashed lines: real values.

Figure 3 shows the temporal evolution of the populations of each mode obtained by numerical integration of the system of equations (11), in two unstable regions of the  $\omega_{4,-}$  branch of the spectrum. The populations are defined as  $N_{m,j}^{u/d}/N_j$ , where  $N_j = f_j N_T$  is the number of particles in component  $j$ ,  $N_T = N_j + N_i$ , and  $f_j$  is the corresponding ratio. As the initial condition, we populate almost equally the  $m = 0$  modes,  $\alpha_{0,j}^{u/d} = \pm\sqrt{N + \delta^{u/d}}$ , and introduce perturbations of order  $\sqrt{N} \cdot 10^{-4}$  for  $m \neq 0$  up to  $m = \pm 5$ . We include the first  $m = \pm 15$  modes in the simulations, thus truncating the system of equations well above the highest relevant mode. In figure 3(a), we see that for  $|\kappa| = 2.2$ ,  $\epsilon = 1$  and  $\epsilon' = 0.4$ , the modes  $m = \pm 2$  are unstable; as expected, their populations grow exponentially, in agreement with the spectrum shown in figure 2(b). Note that the two components share the same temporal evolution and that the positive and negative modes grow with the same population, thus ensuring angular momentum conservation within each component. Figure 3(b) shows the case  $|\kappa| = 1.8$ ,  $\epsilon = 1$  and  $\epsilon' = 0.4$ , in which the modes  $m = \pm 1$  are unstable. We can also observe secondary excitations in modes  $m = \pm 2$  and  $m = \pm 3$ , however, these excitations can not be predicted by the Bogoliubov-de Gennes equations, (16), as these only describe linear excitations, thus, they are only valid for short times and small fluctuations. The time evolution of the main excitation depends on the value of the tunnelling  $|\kappa|$  within the instability region, which determines, for instance, the maximum population the excitation acquires and the time at which it occurs.

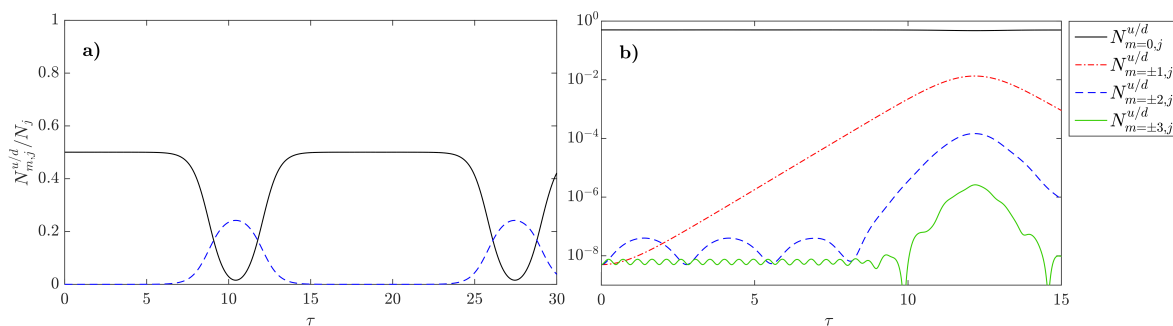


**Figure 3.** (color online). Temporal evolution of the populations of the relevant angular modes in each ring for both components,  $N_{m,j}^{u/d}/N_j = N_{m,i}^{u/d}/N_i$  (with  $f_1 = f_2$ ), in units of  $\tau = \hbar t/2MR^2$ . Initial conditions:  $|\alpha_{0,j}^u|^2 = 0.5005$ ,  $|\alpha_{0,j}^d|^2 = 0.4995$ ,  $\epsilon = 1$ ,  $\epsilon' = 0.4$ ; we add perturbations of order  $\sqrt{N} \cdot 10^{-4}$  in the first  $m$  modes up to  $\pm 5$ , and include  $m = \pm 15$  in the simulation. a)  $|\kappa| = 2.2$ , b)  $|\kappa| = 1.8$ .

## 5. Josephson oscillations and quantum self-trapping

In this section, we study the dynamical regimes of the system for an arbitrary population imbalance between the rings. One-component BECs in double-well systems are known to present either population oscillations between the two wells, known as Josephson oscillations, or quantum self-trapping [28]. First, we study numerically the dynamics of our system when the two components are decoupled, *i.e.*, for  $\epsilon' = 0$ , and only one mode is initially populated,  $m = 0$ .



We define the self-trapping parameter as  $S_m = S_{m,i} = S_{m,j} = (N_{m,j}^u|_{\max,\tau} - N_{m,j}^u|_{\min,\tau}) / (N_{m,j}^u|_{\tau=0} - N_{m,j}^d|_{\tau=0})$ , such that  $S = 1$  for Josephson oscillations and  $S \leq 0.5$  for self-trapping. The left panel in figure 4 shows the  $S$  parameter as a function of the initial population imbalance between rings,  $z_{m,j} = (N_{m,j}^u - N_{m,j}^d) / N_j$ , which is the same for both components, and the ratio between the intra-species nonlinear interactions and the tunnelling,  $\epsilon/|\kappa|$ . The self-trapping regime occurs for sufficiently large imbalance and nonlinear interactions. The right panel in figure 4 shows the evolution of the populations,  $N_{0,j}^{u/d} / N_j$ , in the transition from Josephson oscillations to the self-trapping regime, for  $z_{0,1}(\tau = 0) = z_{0,2}(\tau = 0) = 0.6$  and for different values of the ratio  $\epsilon/|\kappa|$ : a)  $\epsilon/|\kappa| = 4$ , b)  $\epsilon/|\kappa| = 8$ , c)  $\epsilon/|\kappa| = 10$ , d)  $\epsilon/|\kappa| = 24$ . As the nonlinear interactions grow, the oscillations become anharmonic until they are finally suppressed in the self-trapping regime, in which the populations remain trapped in the initial ring. If one further increases  $\epsilon/|\kappa|$ , the amplitude of the remaining oscillations decreases.

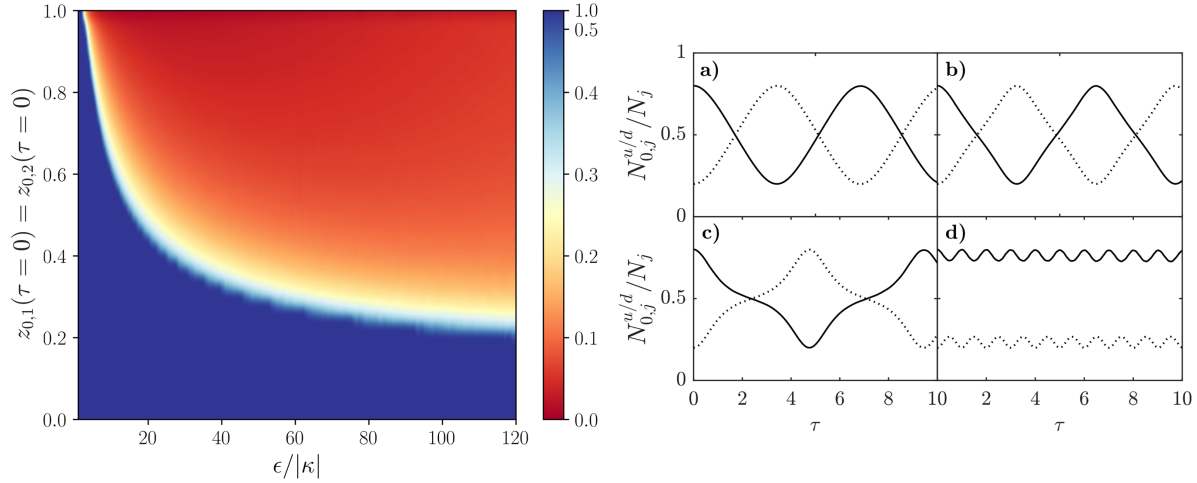


**Figure 4.** (color online). Left: self-trapping parameter  $S$  as a function of the initial population imbalance between the rings,  $z_{0,1}(\tau = 0) = z_{0,2}(\tau = 0)$ , and the ratio between the intra-species nonlinear interactions and the tunnelling  $\epsilon/|\kappa|$ , with  $\epsilon' = 0$  and  $f_1 = f_2$ . Note that the color scale is nonlinear. Right: evolution of  $N_{0,j}^{u/d} / N_j$  (continuous) and  $N_{0,j}^d / N_j$  (dotted) for  $z_{0,1}(\tau = 0) = z_{0,2}(\tau = 0) = 0.6$  and a)  $\epsilon/|\kappa| = 4$ , b)  $\epsilon/|\kappa| = 8$ , c)  $\epsilon/|\kappa| = 10$ , d)  $\epsilon/|\kappa| = 24$ . Both components have the same evolution.

In order to find the self-trapping condition for  $\epsilon' \neq 0$ , we initially populate a single mode  $m$  in each component and factorize the amplitudes as  $\alpha_{m,j}^{u/d} = \sqrt{N_{m,j}^{u/d}} e^{i\beta_{m,j}^{u/d}}$ . The system of equations, (11), can be then written in terms of the population imbalance and the phase difference,  $\delta\phi_{m,j} = \beta_{m,j}^d - \beta_{m,j}^u$ , as a set of four coupled equations (Supplementary Material C):

$$\dot{z}_{m,j} = -\sqrt{1 - z_{m,j}^2} \sin \delta\phi_{m,j}, \quad \delta\dot{\phi}_{m,j} = \frac{1}{2}\Lambda z_{m,j} + \frac{1}{2}\Lambda' z_{m,i} + \frac{z_{m,j}}{\sqrt{1 - z_{m,j}^2}} \cos \delta\phi_{m,j}, \quad (18)$$

where  $\Lambda = \gamma_{jj} N_T / (4\pi|\kappa|)$ ,  $\Lambda' = \gamma_{ji} N_T / (4\pi|\kappa|)$ , with  $N_T$  the total number of particles, and taking  $f_j = f_i$ . Since  $z_{m,j}$  and  $\delta\phi_{m,j}$  are canonically conjugate variables,  $\partial H / \partial z_{m,j} =$

$\delta\dot{\phi}_{m,j}$  and  $\partial H/\partial\delta\phi_{m,j} = -\dot{z}_{m,j}$ , the corresponding Hamiltonian reads [29]

$$H = -\cos\delta\phi_{m,1}\sqrt{1-z_{m,1}^2} + \frac{1}{4}\Lambda z_{m,1}^2 - \cos\delta\phi_{m,2}\sqrt{1-z_{m,2}^2} + \frac{1}{4}\Lambda z_{m,2}^2 + \frac{1}{2}\Lambda' z_{m,1}z_{m,2}. \quad (19)$$

Note that the Hamiltonian is independent of the modes  $m$  that populate each component; thus, the system presents identical dynamics for different values of the total angular momentum. In order to find the condition for simultaneous self-trapping in both components, we impose the initial conditions  $z_{m,1}(\tau=0) = \pm z_{m,2}(\tau=0) \equiv z(0)$  and  $|\delta\phi_{m,1}(\tau=0)| = |\delta\phi_{m,2}(\tau=0)| \equiv \delta\phi(0)$ . Using the initial conditions and imposing energy conservation in (19), for  $z_{m,j}(\tau) = 0$  one reaches (supplementary Material D)

$$\frac{\Lambda \pm \Lambda'}{2} > \left( \frac{\Lambda \pm \Lambda'}{2} \right)_c = 2 \left( \frac{\cos\delta\phi(0)\sqrt{1-z^2(0)} + 1}{z^2(0)} \right), \quad (20)$$

which defines the phase boundary between the two regimes in terms of the population imbalance and the nonlinear interactions. This condition is a generalization of the one found in [30] for a one-component BEC in a double-well potential. The system can present simultaneous self-trapping of the two components in the same well for  $z_{m,1}(\tau=0) = z_{m,2}(\tau=0)$  or in opposite wells, for  $z_{m,1}(\tau=0) = -z_{m,2}(\tau=0)$ . Figure 5 shows the phase boundary defined by (20) for different values of the initial phase difference  $\delta\phi(0)$  as a function of  $(\Lambda + \Lambda')/2 = (\epsilon + \epsilon')/|\kappa|$  and the initial population imbalance  $z_{m,1}(\tau=0) = z_{m,2}(\tau=0)$ . As this phase difference grows from 0 to  $\pi$ , the region of parameters for which self-trapping occurs grows and, as one approaches the limit  $\delta\phi(0) \rightarrow \pi$ , the minimum population imbalance to obtain self-trapping approaches  $z_{m,j}(\tau=0) = 0$ . The numerical values agree with the analytical prediction.

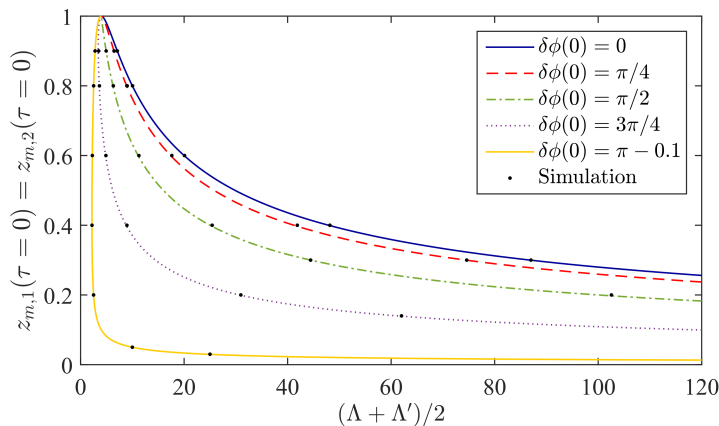


**Figure 5.** (color online). Phase boundary between the self-trapping and the Josephson oscillations regime for different values of the phase difference  $\delta\phi(0)$  as predicted by (20) (lines) and for numerical simulations (points).

## 6. Conclusions

In this work, we have studied the dynamics of a two-component Bose-Einstein condensate in the miscible regime trapped in two rings in ladder configuration. Within the mean field theory, we have derived a few state model for the angular

momentum modes from the two-component Gross-Pitaevskii equation. We have solved the Bogoliubov-de Gennes equations for the stationary states, thus determining the stability regions in the parameter space. Both the inter- and intra-species nonlinear interactions have been found to increase the instability regimes. Also, we have analysed the dynamical behaviour of the system for an arbitrary population imbalance: the transition from Josephson oscillations to quantum self-trapping. In particular, for the case in which a single mode is populated in each component, we have derived the self-trapping condition by deriving a four-state model in terms of the population imbalance between rings and the corresponding phase difference. We have found that the dynamics do not depend on the total angular momentum of the system. The two components present simultaneous self-trapping in the same well or in different wells depending on the initial conditions. In all cases, the analytical results have been corroborated by numerical simulation of the complete set of equations obtaining a very good agreement.

## Acknowledgments

I would like to express my deep gratitude to Dr. Verònica Ahufinger for her constant support and dedication during the development of this work. I also thank Fundació Catalunya - La Pedrera for the scholarship Màsters d'Excel·lència.

## References

- [1] L. Amico *et al.* New J. of Phys. **19**, 020201 (2017).
- [2] J. L. Helm *et al.* Phys. Rev. Lett. **114**, 134101 (2015).
- [3] F. Jendrzejewski *et al.* Phys. Rev. Lett. **113**, 045305 (2014).
- [4] A. Ramanathan *et al.* Phys. Rev. Lett. **106**, 130401 (2011).
- [5] M. Andersen *et al.* Phys. Rev. Lett. **97**, 170406 (2006).
- [6] C. Ryu *et al.* Phys. Rev. Lett. **99**, 260401 (2007).
- [7] A. Turpin *et al.* Opt. Express **23**, 1638 (2015).
- [8] E. M. Wright *et al.* Phys. Rev. A **63**, 013608 (2000).
- [9] B. E. Sherlock *et al.* Phys. Rev. A **83**, 043408 (2011).
- [10] A. S. Arnold, Opt. Lett. **37**, 2505 (2012).
- [11] T. A. Bell *et al.* New J. Phys. **18**, 035003 (2016).
- [12] S. K. Schnelle *et al.* Opt. Express **16**, 1405 (2008).
- [13] K. Henderson *et al.* New J. Phys. **11**, 043030 (2009).
- [14] D. Aghamalyan *et al.* Phys. Rev. A **88**, 063627 (2013).
- [15] I. Lesanovsky *et al.* Phys. Rev. Lett. **98**, 8 (2007).
- [16] X. Zhang *et al.*, Phys. Rev. A **86**, 063628 (2012).
- [17] J. Polo *et al.* New J. Phys. **18**, 015010 (2016).
- [18] C. J. Myatt *et al.* Phys. Rev. Lett. **78**, 586 (1997).
- [19] S. B. Papp *et al.* Phys. Rev. Lett. **101**, 040402 (2008).
- [20] G. Modugno *et al.* Phys. Rev. Lett. **89**, 190404 (2002).
- [21] A. White *et al.* Phys. Rev. A **93**, 033601 (2016).
- [22] F. Malet *et al.* Phys. Rev. A **81**, 013630 (2010).
- [23] X.-F. Zhang *et al.* Sci. Rep. **5**, 8684 (2015).
- [24] E. P. Gross, Phys. Rev. **106**, 161 (1957).
- [25] V. L. Ginzburg *et al.* J. Exptl. Theoret. Phys. (U.S.S.R.) **34**, 1240 (1958).
- [26] T.-L. Ho *et al.* Phys. Rev. Lett. **77**, 3276 (1996).
- [27] N. N. Bogoliubov, J. Phys. (U.S.S.R.) **11**, 23 (1947).
- [28] M. Albiez *et al.* Phys. Rev. Lett. **95**, 1 (2005).
- [29] X. Xu *et al.* Phys. Rev. A **78**, 043609 (2008).
- [30] A. Smerzi *et al.* Phys. Rev. Lett. **79**, 4950 (1997).